

# Detection of a bright feature on the surface of Betelgeuse

D. F. Buscher,<sup>1</sup> C. A. Haniff,<sup>1,2</sup> J. E. Baldwin<sup>1</sup> and P. J. Warner<sup>1</sup>

<sup>1</sup>Mullard Radio Astronomy Observatory, Cavendish Laboratory, Madingley Road, Cambridge CB3 0HE

<sup>2</sup>Palomar Observatory, California Institute of Technology, Pasadena, CA 91125, USA

Accepted 1990 April 18. Received 1990 April 17

## SUMMARY

We present high-resolution images of the M-supergiant Betelgeuse in 1989 February at wavelengths of 633, 700 and 710 nm, made using the non-redundant masking method. At all these wavelengths, there is unambiguous evidence for an asymmetric feature on the surface of the star, which contributes 10–15 per cent of the total observed flux. This might be due to a close companion passing in front of the stellar disc or, more likely, to large-scale convection in the stellar atmosphere.

## 1 INTRODUCTION

The M-supergiant star Betelgeuse ( $\alpha$  Orionis) shows irregular photometric, polarimetric and spectroscopic variability, suggesting the occurrence of complex activity on the star's surface and in its extended atmosphere. Although Betelgeuse has the largest apparent angular size of any star apart from the Sun, direct observation of these phenomena has been prevented by turbulence in the Earth's atmosphere, which limits the angular resolution of conventional ground-based imaging methods to about 1 arcsec, compared with a stellar disc diameter of about 50 milliarcsec (mas). Interferometric techniques, on the other hand, allow details on spatial scales down to the diffraction limit of the telescope to be imaged despite the presence of this atmospheric 'seeing'.

Previous interferometric observations at optical wavelengths have revealed structure in the extended gas and dust envelope around Betelgeuse (Goldberg *et al.* 1981; Roddier & Roddier 1983; Hebden, Eckart & Hege 1988), indicating that the mass loss from the star is neither continuous nor symmetric in nature. So far only tentative evidence (Lynds, Worden & Harvey 1976; Goldberg *et al.* 1981; Hege *et al.* 1982; Hebden *et al.* 1986; Karovska, Nisenson & Noyes 1989) has been put forward for the existence of corresponding asymmetries at the stellar surface. We report here an unambiguous detection of structure on the stellar disc, made using the non-redundant masking (NRM) method (Baldwin *et al.* 1986; Haniff *et al.* 1987).

## 2 OBSERVATIONS

Observations were made in the ground-based high-resolution imaging laboratory (GHRIL) at the Nasmyth focus of the William Herschel Telescope (WHT). The optical setup was similar to that used in previous NRM experiments (Baldwin *et al.* 1986; Haniff *et al.* 1987). The 4.2-m WHT primary mirror was re-imaged with a demagnification by a factor of

190 on a pupil plane mask. The mask was opaque apart from a linear non-redundant array of five 0.52-mm diameter holes, i.e. with effective diameters at the primary of 10 cm. The light emerging through the holes was focused on to a CCD detector at a scale of 16 mas pixel<sup>-1</sup>. This produced a stellar image consisting of an Airy disc crossed by a set of interference fringes at 10 spatial frequencies, the smallest fringe spacing being 38 mas (see Table 1). The array of holes was aligned so that the fringe modulation was along the direction of the CCD serial readout register.

The CCD was operated in a special manner to allow a continuous sequence of short-exposure images to be read out. For each exposure, a 256 × 256 pixel region of the CCD was binned 'on-chip' in the direction orthogonal to the serial readout register and read out as a 256 × 1 pixel projection of the original image. This format preserved the useful information in the image while reducing dramatically the readout time, the total readout noise and the data storage requirements. Exposures were taken at the rate of one every 27 ms; they were collected in data sets of 512 consecutive images.

Four data sets were taken on  $\alpha$  Ori followed by four data sets on a calibration point source,  $\gamma$  Ori. The measurements were repeated with the GHRIL image rotator set to a number of different position angles. This effectively rotated the aperture mask with respect to the sky, thus accomplishing

**Table 1.** Observing parameters for the images presented here. The designation (TiO) indicates that the observing bandpass is inside a TiO absorption feature. The resolution is defined as the spacing of the finest fringes produced by the mask.

Date	$\lambda$ (nm)	$\Delta\lambda$ (nm)	Maximum baseline (m)	Resolution (mas)	No. of position angles
25 Feb 1989	633	12	2.7	48	9
26 Feb 1989	(TiO) 710	10	2.7	54	10
27 Feb 1989	700	10	3.8	38	12
28 Feb 1989	(TiO) 710	10	3.8	39	12

two-dimensional coverage of the spatial frequency plane. Details of the pupil masks and narrow-band filters used are given in Table 1.

### 3 DATA REDUCTION

The data reduction procedure was essentially that described by Haniff *et al.* (1987): the visibility modulus squared for each baseline and the triple product for each closed loop of baselines were calculated on an exposure-by-exposure basis and averaged over all the exposures collected at a given image rotator position angle. The averaged quantities were corrected for photon and readout noise bias. The visibilities were calibrated by dividing the rms source visibilities by the corresponding rms calibrator visibilities. The object closure phases, i.e. the phases of the averaged triple products, did not need calibration since, as expected, the closure phases for the calibrator point source were zero to within the measurement noise. The position angle and the angular scale of the system were calibrated using observations of close binary stars with known orbits.

For Betelgeuse and  $\gamma$  Ori the detected fluxes were approximately  $10^5$  and  $10^4$  photon exposure<sup>-1</sup>, respectively, so the effects of photon and detector noise on the accuracy of the derived amplitudes and closure phases were very small, except at the very highest spatial frequencies. Atmospheric perturbations in the phase of the optical wavefront across the subapertures, and during the exposure time, led to residual errors of about 2° in the closure phases and a fractional error of 2 per cent on the amplitudes for an average of 2000 exposures. Estimated uncertainties of about 10 per cent in the calibrated amplitudes were thought to arise from Betelgeuse not being observed under the same seeing conditions as  $\gamma$  Ori. At the highest spatial frequencies, where Betelgeuse is resolved, the visibility modulus was very small, and the errors on the amplitudes rose to about 20 per cent and those on the closure phases on triangles containing long baselines to about 15°, because of the effects of photon noise.

### 4 RESULTS

Fig. 1 shows the calibrated data for one set of observations (710 nm, maximum baseline 3.8 m). Several features of the brightness distribution over  $\alpha$  Ori can be deduced from these data without detailed analysis. These are as follows.

- (i) The fall in visibility amplitudes with increasing baseline shows that  $\alpha$  Ori is significantly resolved.
- (ii) The large values of closure phases for many baseline triangles and position angles provide unequivocal evidence for strong asymmetry in the brightness distribution (symmetric objects have closure phases of 0° or 180° only).
- (iii) At a position angle of 270° the closure phases all lie within 8° of zero except for those involving the longest baseline, which are close to 180°. This implies that the one-dimensional brightness distribution obtained by integration in strips lying parallel to PA 270° is essentially symmetric, and that the longest baseline lies beyond the first zero of the visibility function. It can be seen in Fig. 1(a) that this is consistent with a natural extrapolation of the visibilities at shorter baselines.
- (iv) The visibility amplitudes at PA 270° give a good fit to those expected from a uniform disc 57 mas in diameter,

although a satisfactory fit is also obtained for various limb-darkened models. Higher quality data would be needed to distinguish such models.

(v) Upper limits to any asymmetry in the brightness distribution in the outer parts of the field of view (e.g. the presence of a stellar companion) are set by the closure phases on the triangle of shortest baselines (213), for which the stellar disc itself is scarcely resolved. The values of the closure phase at different PAs have a mean value of 0.9 with standard deviation 1.3. This sets an upper limit to the flux from a companion of 2–3 per cent of that of  $\alpha$  Ori for radii between 40 and 500 mas from  $\alpha$  Ori.

(vi) The slow and systematic variation of closure phase with PA indicates that the asymmetric component of the brightness distribution lies close to the centre of the distribution, certainly within the radius of the stellar disc. Its magnitude is approximately 10 per cent of the total flux, as deduced from the visibility amplitudes at long baselines where the amplitude of the symmetrical component is small.

The calibrated amplitude and closure phase data were inverted using a standard radio VLBI mapping program which employed a maximum entropy method (Sivia 1987) to reconstruct images of the source. The images shown in Fig. 2(a)–(c) confirm the conclusions of the foregoing analysis, showing a disc with a bright spot towards the west. In addition, the higher resolution images show significant limb-brightening of the disc. Images made from artificial data simulating the observation of a uniform disc with the same non-redundant array also show this limb brightening, but do not show the asymmetric bright spot, indicating that the former feature is an artefact of the image reconstruction process, whereas the latter is not.

Outside the stellar disc, the images show no features with peak brightness of more than 3 per cent of the disc brightness or with more than 1 per cent of the total disc flux in any one feature. Thus we see no evidence for either of the stellar companions detected by Karovska *et al.* (1986, 1989).

Since the resolution of the current observations is insufficient to show any detail in the asymmetry, the position and brightness of the hotspot and the diameter of the star were determined by fitting a model consisting of a uniform disc and a point source to the visibility and closure phase data. The results are summarized in Table 2.

The derived disc diameters are consistent with the reports of previous observers (Balega *et al.* 1982; Cheng *et al.* 1986) that the apparent diameter is greater in the TiO band than in the nearby continuum, and that the apparent diameter at continuum wavelengths increases with decreasing wavelengths, as would be expected from a scattering model for the photosphere.

### 5 CONCLUSIONS

We have detected a hotspot on Betelgeuse at a very high level of confidence. It should be noted that this result can be inferred from visual inspection of the visibility and closure phase data alone: the image reconstruction serves mainly to confirm the conclusions from this inspection and from the model-fitting. Since image reconstruction can be viewed as a process of model-fitting, where the number of degrees of freedom is of the order of the number of pixels in the map, it allows one to see if there is any other brightness distribution

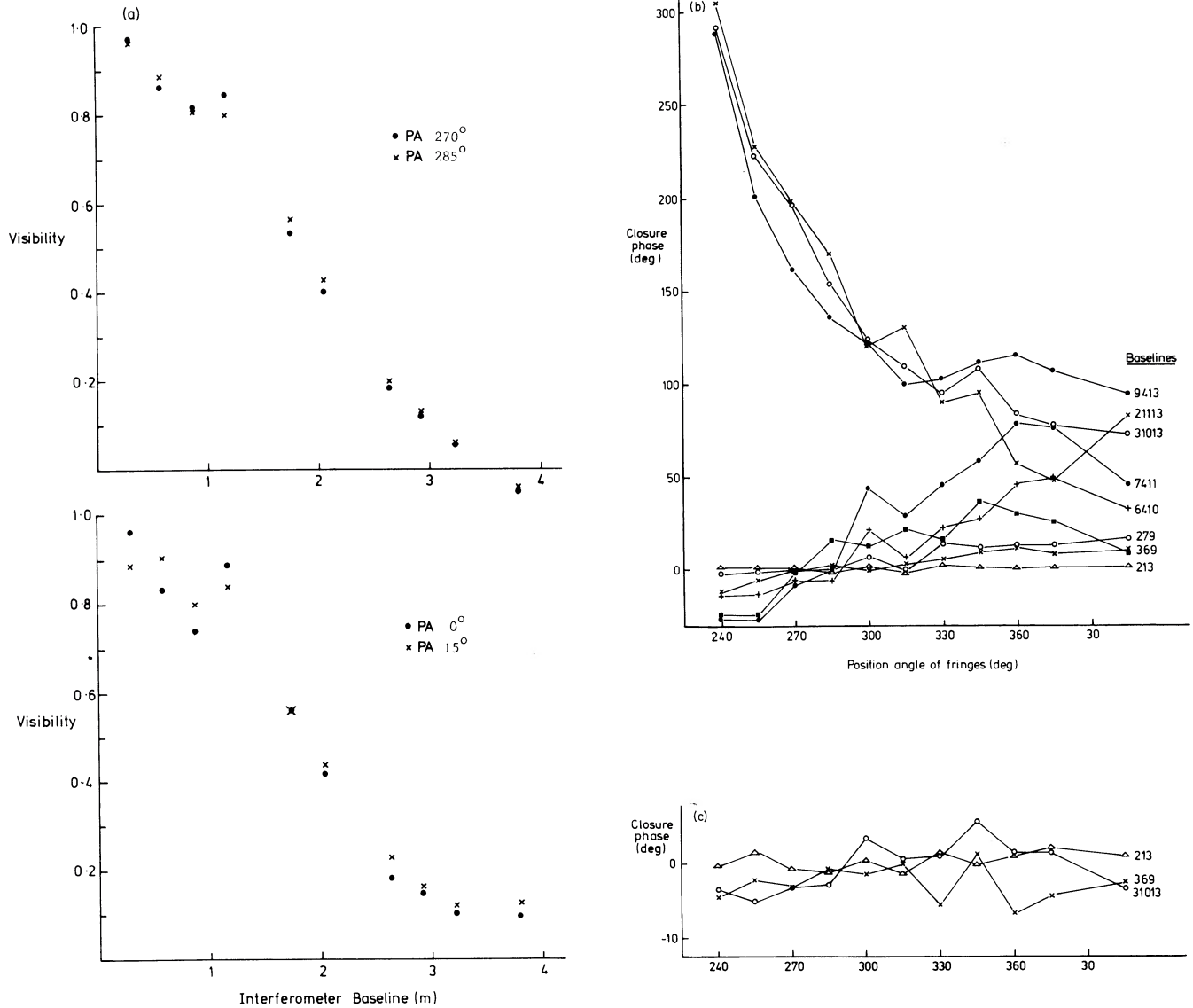


**Figure 1.** Calibrated visibility amplitude and closure phase data for the 710-nm, 3.8-m maximum baseline observation. This five-hole mask produces baselines of 1, 2, 3, 4, 6, 7, 9, 10, 11, 13 times 29 cm. In (a) the amplitudes are shown as a function of baseline for four position angles of the mask, while in (b) and (c) the closure phases are plotted as a function of position angle. The closure phases are labelled by concatenating the indices of the three contributing baselines. Graph (b) shows the closure phases measured for Betelgeuse, while graph (c) shows those measured for the calibration point source  $\gamma$  Ori. Note the change of vertical scale between (b) and (c). Only a subset of the closure phases are plotted in (c), for clarity.

which could adequately fit the data. Parameters of the disc and hotspot were obtained by fitting the data with a simple model.

No definite conclusions as to the nature of the hotspot can be made. Possible explanations include a stellar companion passing in front of the supergiant's disc or differential photospheric brightening due to the effects of stellar rotation. Perhaps the most favoured model used to explain the observed polarization and variability of Betelgeuse (Schwarz & Clarke 1984; Hayes 1984) is that of large-scale convective features on the stellar surface, as suggested by Schwarzschild (1975).

These surface zones are expected to be so large that only a few would be present on the surface at any one time, and their predicted brightness is consistent with our observa-

**Table 2.** Disc and point source parameters from model-fitting (see text). The quoted errors are the 95 per cent confidence limits, i.e. approximately twice the rms error.

Observation wavelength(nm)/ resolution(mas)	Disc Diameter (mas)	Point Source Parameters		
		Flux (% of total)	Radius from centre (mas)	PA (degrees)
633/48	61( $\pm$ 4)	15(+3/-5)	6(+2/-1.5)	277( $\pm$ 6)
700/38	54( $\pm$ 2)	14(+2/-1)	4( $\pm$ 1)	281( $\pm$ 4)
710/39	58( $\pm$ 2)	10( $\pm$ 2)	8( $\pm$ 1.5)	276( $\pm$ 6)
710/54	61(+8/-4)	15(+9/-6)	6(+4/-2)	276( $\pm$ 7)

tions. Indeed our data do suggest that we are seeing an asymmetry arising very close to the stellar surface, since the hotspot shows a similar amount of obscuration by TiO as the rest of the photosphere.

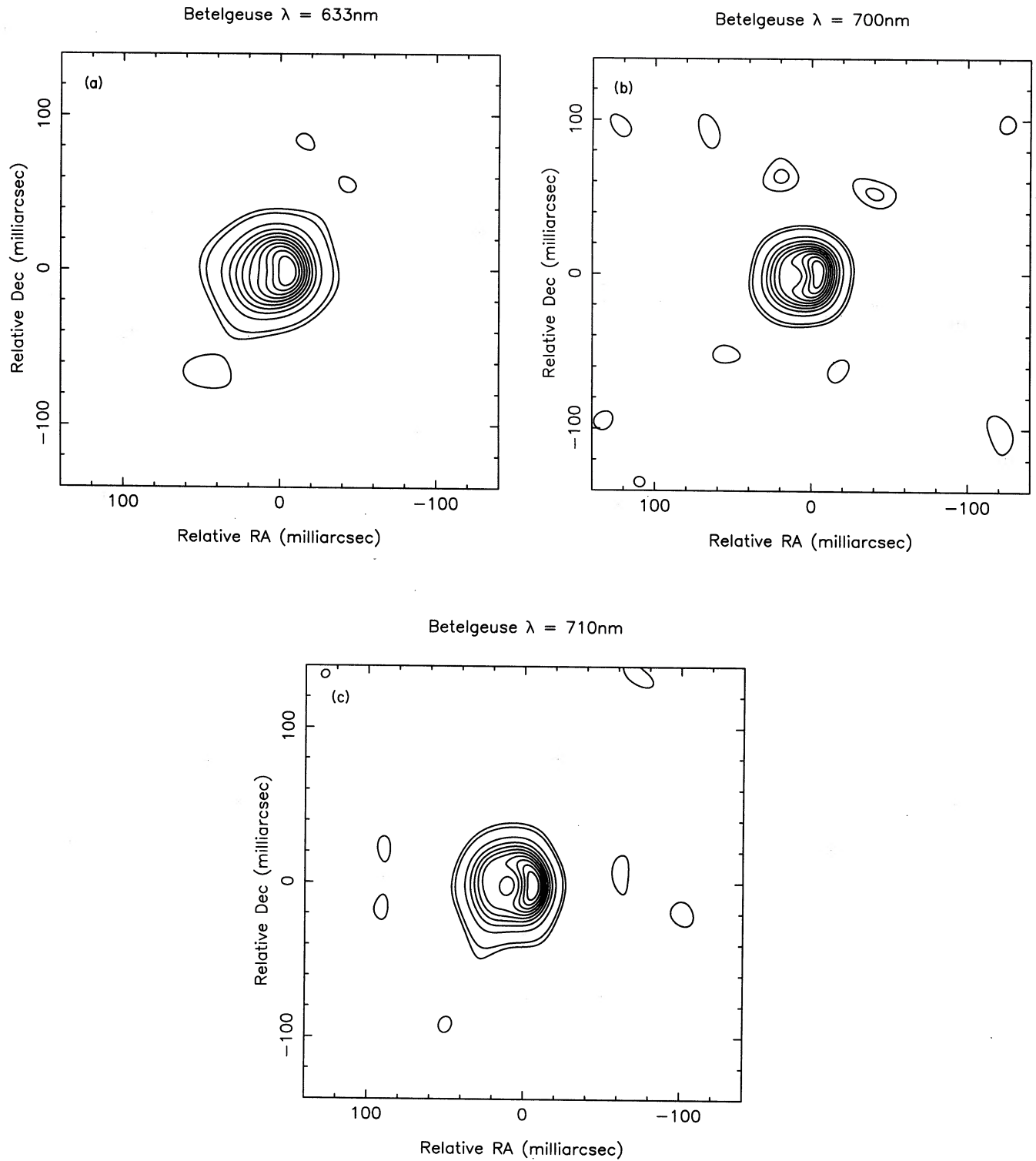


**Figure 2.** Reconstructed images of Betelgeuse at wavelengths of (a) 633 nm, (b) 700 nm and (c) 710 nm, with resolutions of 48, 38 and 39 mas, respectively. The contour levels are at 1, 2, 10, 20, 30, ... 80, 90 per cent of the peak brightness. The images show a moderate amount of ‘super-resolution’, because the maximum entropy algorithm used to reconstruct them allows *a priori* constraints, such as positivity and finite extent of the image, to be enforced. The spots outside the central disc are consistent with the expected noise level.

The detailed understanding of this hotspot has clearly only just begun. Schwarzschild (1975) suggests that the evolution time of convective cells may be as short as 200 d. Rotation time-scales are likely to be very much longer.

Quantitative statements about its temperature and evolution will require further high-quality interferometric observations to be made over a wider range of wavebands and over several epochs.

## ACKNOWLEDGMENTS

Generous financial support was provided by the Royal Commission for the Exhibition of 1851 (DFB) and by Christ's College, Cambridge (CAH), in the form of a Research Fellowship. We thank Craig Mackay for advice on the operation of the CCD. The WHT is operated by the Royal Greenwich Observatory at the Observatorio del Roque de los Muchachos of the Instituto de Astrofísica de Canarias.

## REFERENCES

- Baldwin, J. E., Haniff, C. A., Mackay, C. D. & Warner, P. J., 1986. *Nature*, **320**, 595.
- Balega, Y., Blazit, A., Bonneau, D., Koechlin, L., Foy, R. & Labeyrie, A., 1982. *Astr. Astrophys.*, **115**, 253.
- Cheng, A. Y. S., Hege, E. K., Hubbard, E. N., Goldberg, L., Strittmatter, P. A. & Cocke, W. J., 1986. *Astrophys. J.*, **309**, 737.
- Christou, J. C., Hebden, J. C. & Hege, E. K., 1988. *Astrophys. J.*, **327**, 894.
- Goldberg, L., Hege, E. K., Hubbard, E. N., Strittmatter, P. A. & Cocke, W. J., 1981. In: *Second Cambridge Workshop on Cool Stars, Stellar Systems and the Sun*, p. 131, eds Giampapa, M. S. & Golub, L., SAO Spec. Rep. No. 382.
- Haniff, C. A., Mackay, C. D., Titterton, D. J., Sivia, D., Baldwin, J. E. & Warner, P. J., 1987. *Nature*, **328**, 694.
- Hayes, D. P., 1984. *Astrophys. J. Suppl.*, **55**, 179.
- Hebden, J. C., Eckart, A. & Hege, E. K., 1987. *Astrophys. J.*, **314**, 690.
- Hebden, J. C., Christou, J. C., Cheng, J. Y. S., Hege, E. K. & Strittmatter, P. A., 1986. *Astrophys. J.*, **309**, 745.
- Hege, E. K., Hubbard, E. N., Strittmatter, P. A. & Cocke, W. J., 1982. *Opt. Acta*, **29**, 701.
- Karovska, M., Nisenson, P. & Noyes, R., 1986. *Astrophys. J.*, **308**, 260.
- Karovska, M., Nisenson, P. & Noyes, R., 1989. *Bull. Am. astr. Soc.*, **19**, 755.
- Lynds, C. R., Worden, S. P. & Harvey, J. W., 1976. *Astrophys. J.*, **207**, 174.
- Roddier, C. & Roddier, F., 1983. *Astrophys. J.*, **270**, L23.
- Schwarz, H. E. & Clarke, D., 1984. *Astr. Astrophys.*, **132**, 370.
- Schwarzschild, M., 1975. *Astrophys. J.*, **195**, 137.
- Sivia, D. S., 1987. *PhD thesis*, Cambridge University.